Eur J Vasc Endovasc Surg (2020) 59, 625–634

Infrared Illumination and Subcutaneous Venous Network: Can it be of Help for the Study of CEAP C_1 Limbs?

Francisco Ortega-Santana [a,b,*], **Pablo Hernández-Morera** [c], **Fátima Ruano-Ferrer** [b], **Aritz Ortega-Centol** [b,d]

[a] Department of Morphology, University of Las Palmas de Gran Canaria, Edificio Ciencias de la Salud, Las Palmas de Gran Canaria, Spain
[b] CliniVar, Clínica de Varices, Las Palmas de Gran Canaria, Spain
[c] IUMA Information and Communication Systems, University of Las Palmas de Gran Canaria, Edificio Electrónica y Telecomunicación, Las Palmas de Gran Canaria, Spain
[d] Universitary Hospital of Bellvitge, L'Hospitalet de Llobregat, Barcelona, Spain

WHAT THIS PAPER ADDS

This observational research demonstrates quantitatively that near infrared illumination increases the visualisation of the subcutaneous venous network between 2.6 and 16.2 times *vs.* the traditional system of visual inspection. Morphological details of the superficial venous network of the lower extremities are more clearly displayed than with the naked eye, which allows for future studies to be designed to obtain better knowledge of the superficial venous network. This could be of help in understanding the behaviour in both control limbs (CEAP C_{0A} class) and limbs with venous incompetence (classes C_{0S} and C_1 of the CEAP classification).

Objective: The subcutaneous venous network (SVN) is difficult to see with the naked eye. Near infrared illumination (NIr-I) claims to improve this. The aims of this observational study were to investigate whether there are differences between the different methods; to quantify the length and diameter of SVNs; and to confirm if they differ between C_{0A} and C_1 CEAP limbs.

Methods: In total, 4 796 images, half of them from the visible spectrum (VS) and the other half from the nearninfrared spectrum (NIrS), belonging to 109 females (C_{0A}: $n = 50$; C_1 CEAP: $n = 59$) were used to establish the morphological characteristics of the SVN by visual analysis. With Photoshop CS4, SVN diameters and lengths were obtained by digital analysis of 3 052 images, once the images of whole extremities were excluded.

Results: On NIr-I, the diameters, trajectories, and colouration of SVNs of C_1 limbs appeared more irregular than SVNs of C_{0A} limbs. Compared with the VS images, NIr-I allowed visualisation of a greater length of the SVN in both groups ($p < .010$). This capacity varied from 2.6 ± 0.9 times (C_1) to 16.2 ± 11.9 (C_{0A}). While the SVN length seen in the VS images from C_1 limbs was greater than observed in C_{0A} limbs ($p < .001$), differences between NIr-I images only existed in the lateral part of the lower leg ($p = .016$). With NIr-I, the median diameter of the C_1 CEAP SVN veins was 5.8 mm (interquartile range [IQR] 4.3–7.5 mm), while the median diameter in C_{0A} SVN limbs was 2.6 mm (IQR 2.0–3.6 mm) ($p < .001$).

Conclusion: The NIr-I reveals the characteristics of the SVN better than the naked eye. Further studies are required to determine the significance of the changes in the SVN in C_{0A} and C_1 limbs, and the factors causing them.

Keywords: C_{0A} limbs, C_1 limbs, Near-infrared illumination, Subcutaneous veins visualisation
Article history: Received 5 April 2019, Accepted 27 November 2019, Available online 31 January 2020

INTRODUCTION

Chronic venous disease (CVD) is defined as "any morphological and functional abnormality of the venous system of long duration manifested either by symptoms and/or signs",[1] and duplex ultrasound is recommended to identify the source and patterns of reflux.[2] However, the study of the subcutaneous venous network (SVN) is usually not considered an indication for duplex ultrasound investigation.[3] Only occasionally has it been used to show the intimate connections between reticular veins and telangiectasias,[4] or to detect reflux in the dermal microcirculation of subjects with CVD.[5]

Reticular veins are part of the SVN, an intricate network of venous polygons located at different depths from the skin surface,[6,7] and CEAP C_1 class is defined by the presence

* Corresponding author. Department of Morphology, University of Las Palmas de Gran Canaria, Edificio Ciencias de la Salud, Avda. Marítima del Sur S/N, 35016 Las Palmas de Gran Canaria, Spain.
E-mail address: francisco.ortega@ulpgc.es (Francisco Ortega-Santana).

https://doi.org/10.1016/j.ejvs.2019.11.034

of visible telangiectasias and reticular veins between 1 and 3 mm in diameter, measured with the patient in the upright position and detected at a distance of two metres.[1,8] C_1 is therefore produced by alteration of the SVN, but, despite its high prevalence,[9–11] the morphological venous alterations are documented only by the naked eye or by photographs taken in the visible light spectrum. This allows for the visualisation of telangiectasias, but often the reticular veins remain hidden.[12]

Therefore, it would be desirable to have a non-invasive method that allows for the visualisation of the SVN and obtaining information on its characteristics. At the same time, this method should be easy to use in the direct care of patients (level 1 or level 2 of research).[1]

De-oxyhaemoglobin can absorb light at wavelengths close to 800 nm (near infrared). This provides a good contrast between subcutaneous veins and the surrounding tissue, which can be photographed.[13] Different devices use this absorption property,[14] but they only scan a small surface area of about 7–10 cm^2. They do not allow illustration of the SVN distribution in areas such as the thigh or lower leg. Near infrared illumination (NIr-I) allows visualisation of the subcutaneous veins of large body areas,[15] and it has been used to study some aspects of the venous incompetence.[16,17] However, the characteristics of the SVN seen with NIr-I have not been described and objective data provided by this method are not available.

OBJECTIVES

The first objective was to compare quantitatively visual and near infrared (NIr) imaging of the SVN of broad areas of the lower extremities from C_{0A} and C_1 limbs using a new methodology of measuring the length and the diameter of the SVN vessels. The second objective was to describe the morphological characteristics of the SVN for both groups of limbs.

MATERIALS AND METHODS

This observational study was carried out at CliniVar, a phlebology centre associated with the Las Palmas de Gran Canaria University. This work complied with the requirements for medical research[18] and the Declaration of Helsinki, and was approved by the local ethics committee. All patients provided written informed consent. Participants enrolled were seen between January 2016 and December 2017.

Participants, and inclusion and exclusion criteria

The study included 109 patients aged >18 years, divided into two groups (Fig. 1).

Patient group. Fifty-nine consecutive women (mean ± standard deviation [SD] age 39.5 ± 2 years [range 30–47 years]) who requested treatment for primary CVD and were classified as CEAP class C_1 for both limbs after physical examination and a duplex ultrasound were included in the patient group.[1,8]

Control group. Fifty physically active female volunteers (mean ± SD age 25.4 ± 5 years [range 19–32 years]), in whom the presence of any sign or symptom related to venous incompetence was ruled out after a detailed clinical history, physical examination, and duplex ultrasound,[1,8] were included in the control group (CEAP class C_{0A}).

Exclusion criteria. Exclusion criteria included patients with C_{0S} limbs (i.e., those with venous disease related symptoms in at least one limb, but without visible signs of venous diseases);[1,8] reflux in saphenous trunks and tributaries detected by duplex ultrasound; a previous history of deep or superficial venous thrombosis; previous treatment of venous incompetence (surgery or sclerotherapy); hormonal therapy; pregnancy; and other severe diseases not related to CVD.

Image acquisition

Two IDS UI-1490LE cameras (IDS Imaging Development Systems, Obersulm, Germany) equipped with a 10.5 Mpx CMOS sensor, incorporating a 16 mm optics, ½" F 1.8 M12 Stor, were used. One of the cameras captures images in the visible spectrum (VS) of light (400–700 nm), while the second camera captures images in the infrared spectrum

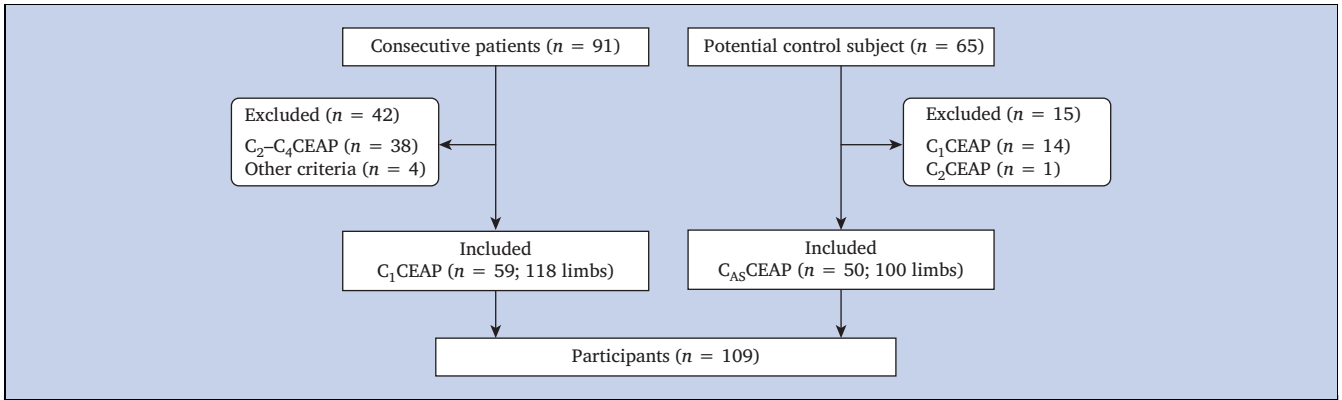

Figure 1. Flow chart showing patient selection. After both a clinical history and detailed investigation, including venous duplex ultrasound of the lower extremities, a total of 109 participants (50 controls with both lower limbs classified as CEAP C_{0A} and 59 patients, also with both lower limbs classified as CEAP C_1), were included in the study. Therefore, a total of 218 lower extremities (100 CEAP class C_{0A} and 118 class C_1) were studied.

(IrS) (>750 nm) thanks to the installation of an infrared long-pass filter (LP695-S33; Midwest Optical Systems, Palatine, IL, USA). The cameras were connected to a computer and their position regulated in order to achieve image matching. The UEye program, provided by the manufacturer, shows the images in real time (Fig. 2).

The VS illumination of the examination room consisted of six Osram L36W/765 fluorescent tubes (Daywhite colour temperature). NIr-I was obtained by two non-focused light bulbs radiating at a wavelength of 850 nm (model IGV-IRCM80-1; IGreenView Optoelectronic Co., Ltd, Shenzhen, China). It has been demonstrated that the range between 800 and 850 nm is optimum to get the best NIr venous image quality for each skin tone.[19]

The participants remained standing and they were required to show their lower extremities. Forty-four images were captured, including the total length of the anterior, medial, posterior, and lateral sides, and detailed images of the thigh (anterior [ATh], medial [MTh], posterior [PTh], and lateral [LTh]) and lower leg (medial [ML], posterior [PL], and lateral [LL]). A total of 4 796 images were collected, half of them obtained in the VS and the other half in the IrS.

Image analysis

Morphological characteristics. Each VS image was visualised paired with its corresponding IrS image (Fig. 3A, D; Figs. S1 and S2 [Supplementary Material]). This allowed the verification of whether the IrS images showed a more extensive SVN than the VS image and appreciation of morphological characteristics among groups, in a non-quantitative way.

Digital analysis and measurement protocol. Images of the entire limb were excluded from digital analysis given that those obtained from the thigh and the leg showed the information in greater detail. Therefore, the final number of images used for statistical purposes was 3 052. All vein measurements were made by two different observers and the reliability of their measurements was determined statistically. The measurements were obtained with a pen tablet (Intuos Draw, Wacom; Wacom Technology, Portland, OR, USA) and the "analysis" tool of the Adobe PhotoShop CS4 Extended program (Adobe System Software Ireland, Dublin, Ireland), according to the following procedure.

SVN length. Each of the anatomical regions were drawn for each one of the coupled VS and IrS images (Fig. 3B). Their extent was measured and expressed as the total number of pixels within the marked area (A_{region}).

The observers manually drew a one pixel thick line along the axis of each visualised vein inside the limits of the delimited areas (Fig. 3C, D). The sum of the lengths of all traced axes represented the total length of the visualised SVN,[20] expressed in pixels (SVN_{region}).

The percentage that the SVN_{region} represented in relation to the anatomical region was calculated as $SVN\text{-}L = (SVN_{region} *100)/A_{region}$ (see Supplementary Material).

Vein diameter. Vein diameters in the SVN were measured only in the infrared images. A grid with squares, each with an area of 150 pixel squares, was superimposed on the IrS images. Up to 10 of the best contrasted and wider tributaries were selected. In each of these squares the vessel, which was determined by its size and trajectory to be the main venous axis of the SVN in that area, was marked. If there were tributaries to this vessel, then the vessel could be marked at each side of this. Vessel diameters were measured at these marks (Fig. 4) by both observers. The diameters were measured as pixels and converted to millimetres by comparison with a 2 cm scale marker, which was placed on the skin of the extremity in some reference images (see Supplementary Material).

Statistical analysis

Data were analysed using SPSS 24.0 (IBM, Armonk, NY, USA). The normality of the sample was tested using the Kolomogorov–Smirnov test with Lilliefors correction, which showed that the data significantly deviated from the normal distribution, so non-parametric tests were used. The median was the statistical value used to determine whether there were significant differences between groups. The Wilcoxon

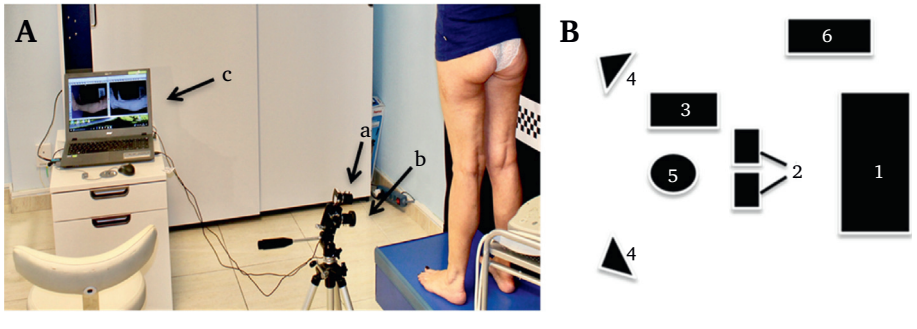

Figure 2. Patient position and distribution of the elements used to obtain both the visible spectrum and the infrared spectrum images. (A) While the patient remains standing, images are obtained with both the (a) visible and (b) infrared spectrum cameras. The images are shown in real time on the (c) computer screen and, if possible, sent to a television screen. (B) 1 = patient position; 2 = visible spectrum and infrared spectrum cameras; 3 = computer; 4 = infrared bulbs; 5 = observer position; 6 = television screen.

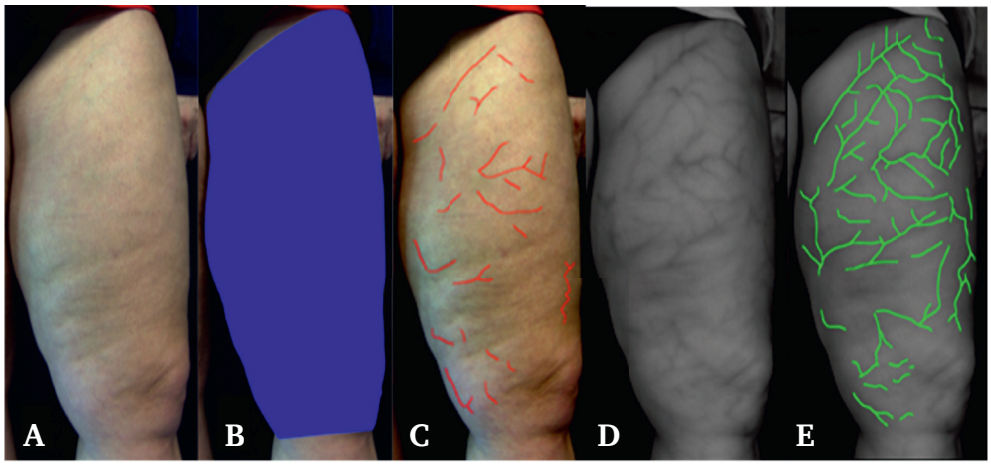

Figure 3. Example of how the total area to be studied is outlined and how the visible vein axes are marked. This image shows how the anatomical area is outlined and how the visible subcutaneous venous network (SVN) is marked for measurement. (A, D) Visible spectrum (VS) and infrared spectrum (IrS) paired images are showed at the same time on screen (see Fig. 1 and Supplementary Material). The upper limit of the thigh can be the inguinal fold, the lower edge of the clothes, or the shadow borders that hinder the visualisation of the SVN. (B) The lower limit of the thigh is drawn between the lower edge of the patella and the popliteal fold. The upper limit of the lower leg is the lower limit of the thigh area, while its lower limit is defined bythe plane passing through the lower edge of the malleoli and the anterior fold of the ankle. The areas are marked in each of the VS and IrS images. (C, E) Two different observers draw one pixel lines over the visible veins, as axes. The sum of these axes represents the length of the SVN. In order to avoid bias, measurements are not taken in places where the presence of shadows or the contrast with the surrounding area did not allow the identification of a vein. The lines have a diameter of 10 pixels, which allows the best visualisation of the images.

test was used for paired comparison between the percentage of the SVN visualised in VS and IrS images, and the Mann—Whitney *U* test for independent samples was used to determine the significance of differences in the medians between data from the control and patient group. A p value of $< .05$ was accepted as significant.

The intraclass correlation coefficient was used to compare the measurements obtained by two observers

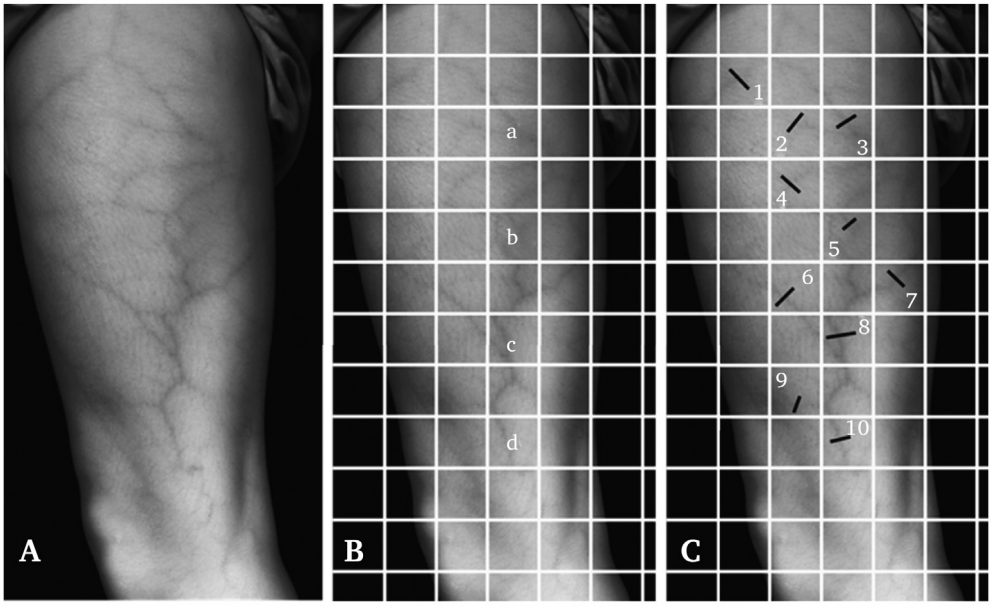

Figure 4. Method used to select the veins for diameter measurement. Over an (A) infrared image, a (B) grid with 150 pixel squares is superimposed. Then, (C) up to 10 of the best contrasted veins are marked (black bars), which must be distributed throughout the region to be studied. When one of the tributaries seems to be the central axis of the SVN in that area (A) it can be marked more than once (B, a—d; C 3, 5, 8, 10). The observers measure the diameters perpendicular to the venous axes and as close as possible to the marks in order to minimise the differences between their results.

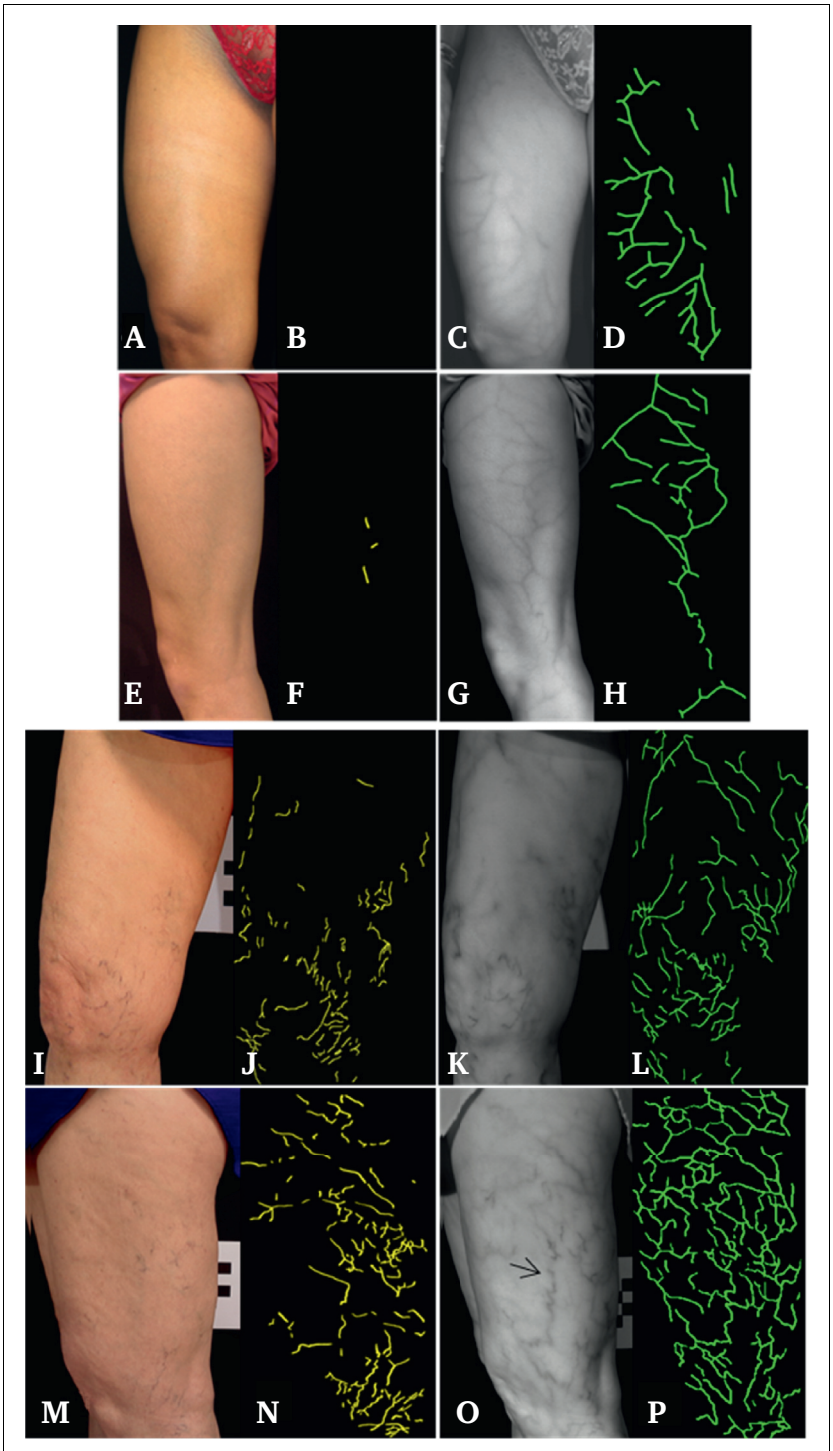

Figure 5. Images of both the visible spectrum (VS) and the infrared spectrum (IrS), grouped by C_{0A} limbs and C_1 limbs. C_{0A} limbs: in the (A, E) VS images, with the naked eye there are no visible telangiectasias and (F) only few normal reticular veins can be observed on the lateral side of the thigh. (C, G) On the paired IrS images it can be seen how the veins of the subcutaneous venous network have a rectilinear course, (D, H) how they tend to form polygonal shapes of different sizes, and how their diameters and their contrast with the neighbouring tissue are uniform. C_1 limbs: in this case, (I, M) telangiectasias and/or reticular veins are visible to the naked eye, which is highlighted when the (J, N) venous axes are traced. (K—P) Infrared images show subcutaneous veins with an irregular course, multiple polygonal connections, and different diameters and contrast intensities. Note how (O, arrow) some subcutaneous veins revealed by infrared illumination join two visual pathological regions, which are apparently independent.

(lengths and diameters) and values > 0.75 were accepted as highly reliable. In order to give greater consistency to the results, the highest values obtained by each one of the observers in the C_{0A} group and the lowest values obtained in the C_1 group were used for statistical analysis (see Supplementary Material).

RESULTS

Morphological characteristics

In control limbs there were no telangiectasias or pathological reticular veins visible on VS images, but they were always seen in CEAP C_1 limbs (Fig. 5A, E, I, M). By contrast, the IrS images, both in control and C_1 limbs, all showed either total or partial SVNs and their different morphological characteristics (Fig. 5C, G, K, O).

Control group

In general, the SVN showed a rectilinear path and their contrast was quite homogeneous, although it varied between limbs. Occasionally, a venous segment was highlighted and presented a sinuous path. The size of the venous polygons, by which the SVNs are organised, varied among individuals: in some cases they were scarce and wide, and in others they were small and numerous. On other occasions it was not possible to appreciate a network and at other times a collateral seemed to be the central axis of the SVN in some of the regions (Fig. 5A—H; Figs. S1, S3, and S4 [Supplementary Material]).

CEAP C_1 group

The SVN can follow a pattern similar to that observed in the control limbs and it was seen more clearly with NIr-I (Figs. 3 and 5), even in those with Fitzpatrick skin type V (Fig. S5; Supplementary Material). In general, the SVN of C_1 limbs has a tendency to form networks of small venous polygons and may have irregular diameters, trajectories, and colourations. Both the quantity and the intensity with which the veins are contrasted differ between the anatomical regions and limbs. Although the SVN alterations shown with NIr-I generally correspond to areas of telangiectasia or pathological reticular veins observed with the naked eye, they are also often seen in areas without venous alterations and joining two or more pathological regions that are apparently independent (Fig. 5I — P).

Digital image analysis

After confirming the reliability of the measurements obtained by the observers (correlation coefficient 0.91 for the diameters and 0.79 for the lengths), statistical analysis was performed.

SVN length (SVN-L). Compared with the VS images, the length of the SVN seen by NIr-I was much greater, both in each region and in each group of limbs (Table 1). However, the visualisation differed between the groups. Calculating how many times the display of the SVN was increased by the use of NIr-I (*SVN-L* IrS/*SVN-L* VS), it has been shown that it did so an average of 16.2 ± 11.9 times in the case of the C_{0A} limbs, whereas in the case of CEAP C_1 limbs the difference between veins visible to the naked eye and those seen by NIr-I only increased 2.6 ± 0.9 times.

When comparing the *SVN-L* seen in each anatomical region by visible light and by infrared light (Fig. 6), the data indicate that the *SVN-L* observed in the VS images was higher in CEAP C_1 limbs than in the control limbs in all the regions studied

Table 1. Percentages of superficial venous network from each anatomical area and each group of limbs (data expressed as pixels)

Anatomical area	C_{0A} group (n = 100 limbs)			C_1 group (n = 118 limbs)		
	Median (IQR) — pixels	Increase — %	p value	Median (IQR) — pixels	Increase — %	p value
Anterior thigh						
Visible spectrum	0.00 (0—0)	±186	<.001	0.31 (0.14—0.89)	6.64	.002
Infrared spectrum	1.86 (1.37—2.71)			2.06 (0.70—2.64)		
Medial thigh						
Visible spectrum	0.00 (0—0)	±253	<.001	0.59 (0.08—1.39)	4.13	.002
Infrared spectrum	2.53 (1.57—3.67)			2.44 (1.22—3.78)		
Lateral thigh						
Visible spectrum	0.04 (0.00—0.36)	60.00	<.001	0.88 (0.27—1.99)	1.84	.036
Infrared spectrum	2.40 (1.68—3.75)			1.62 (1.13—2.90)		
Posterior thigh						
Visible spectrum	0.11 (0.00—0.60)	28.72	<.001	1.24 (0.49—1.70)	2.18	.003
Infrared spectrum	3.16 (1.60—4.35)			2.70 (2.42—4.48)		
Lateral lower leg						
Visible spectrum	0.00 (0—0)	±196	<.001	1.65 (0.70—2.39)	1.91	.001
Infrared spectrum	1.96 (1.41—2.52)			3.16 (1.55—4.17)		
Medial lower leg						
Visible spectrum	0.00 (0—0)	±277	<.001	1.52 (0.92—1.99)	1.99	< .001
spectrum	2.77 (1.98—3.26)			3.02 (2.36—3.88)		
Posterior lower leg						
Visible spectrum	0.14 (0.03—0.43)	13.29	<.001	1.27 (0.55—1.72)	2.35	.005
Infrared spectrum	1.86 (1.13—2.99)			2.98 (2.06—3.51)		

IQR = interquartile range.

($p < .001$). However, when comparing the IrS images of both groups, two differences were apparent: firstly, statistically significant differences only exist in the lateral part of the leg ($p = .016$); secondly, it is striking that, although there were almost no differences between groups within the IrS, the values obtained in the thigh tended to be higher in the control limbs, while, conversely, the median values were somewhat greater in the lower leg level C_1 limbs.

The comparison of the *SVN-L* obtained in the same projections of adjacent anatomical areas of each one of the groups (medial, lateral and posterior from both the thigh and the lower leg) showed that, except in the lateral aspect of the C_{0A} limbs, the *SVN-L* is different in both groups ($p < .010$) (Fig. 7).

Vein diameter. Vein diameters were measured only with IrS images. In C_1 limbs the mean value of the median SVN diameter (5.9 $\pm$ 0.5 mm) was twice that of the C_{0A} limbs (2.8 $\pm$ 0.4 mm) and the SVN diameters of the C_1 limbs were higher than those of the C_{0A} limbs in all areas ($p < .001$). There was variation in the regions, but median size was greatest in the MTh (3.3 mm) and the PL (3.2 mm) for C_{0A} limbs, whereas in C_1 limbs the medians varied between 5.3 mm (PTh, PL) and 6.6 mm (ATh) (Table 2).

DISCUSSION

Since 1933 NIr-I has been used to study venous disorders, but it became an unused technique.[21,22] However, today NIr-I is used to perform venepunctures in difficult patients.[14,21,23,24]

Reticular veins form a complex network,[25] and their alterations are taken into account to classify CEAP C_1 limbs.[8] However, whether the ability of NIr-I to highlight the SVN differs between C_{0A} and C_1 CEAP limbs has not been quantified. Whether morphological vein characteristics are different or if the behaviour of the SVN differs in different anatomical areas is also unknown. Perhaps this has not been studied because the C_1 CEAP class is mainly considered to be a cosmetic problem. Consequently, the methodology and results herein cannot be compared with others.

The data in Table 1 confirm that NIr-I allows visualisation of a greater length of SVN, compared with what has been accepted previously.[15,22,26] The *SVN-L* shown in VS images from C_1 limbs are bigger than those of the control group and these differences were significant in all the regions, which was predictable according to the CEAP classification criteria for a class C_1 diagnosis.[1,8] However, although the values obtained in both groups with NIr-I were higher than those seen in the VS, significant differences were only present on the lateral aspect of the lower leg (Fig. 6).

The present data confirm that NIr-I increases the visualisation and characterisation of the SVN. This is greatest in control limbs where the SVN diameters are smaller and are less readily seen. The NIr-I enhancement also occurs in C_1 limbs but to a lesser extent as these SVN veins are larger and many are already visible. Consequently, NIr-I is an excellent method with which to assess the SVN and should be used to define what is normal and abnormal.

By contrast, in C_1 limbs, NIr-I always allows visualisation of some pathological reticular veins whose main characteristics are a highly contrasted appearance, tortuosity, and larger diameter (Fig. 5). They usually coincide with venous changes seen visually, but NIr-I shows that they are more extensive and can go into areas where there are no appreciable changes in the VS images, or they may join two apparently independent areas with visible pathological veins.

Pathological reticular veins are defined as “dilated bluish subdermal veins, usually 1 mm to less than 3 mm in diameter, usually tortuous”,[1] appreciated by the naked eye

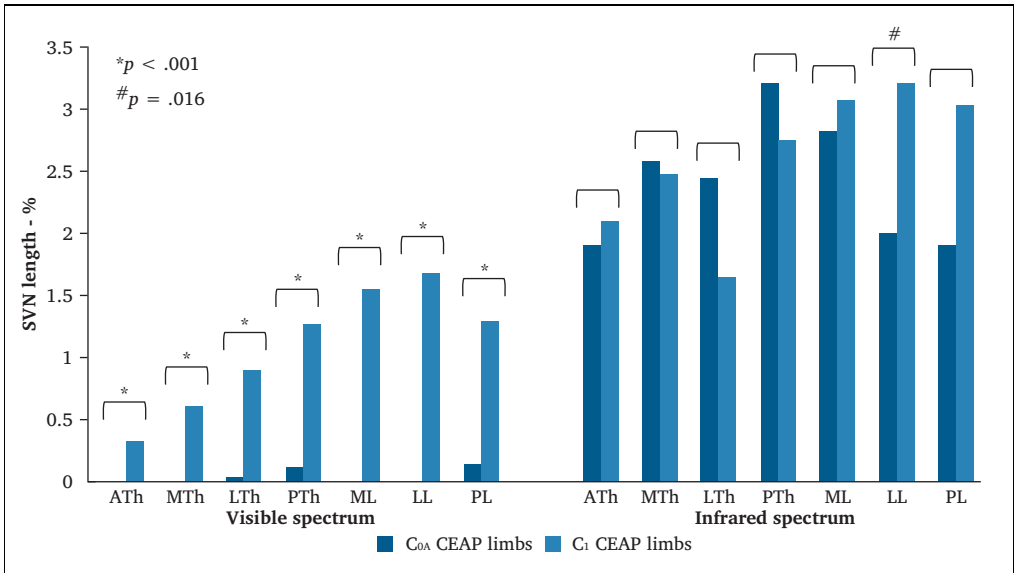

Figure 6. Graphical representation of the percentage of subcutaneous venous network (SVN) seen in relation to each anatomical region grouped by both CEAP class and by light spectrum (values expressed as medians). The length of the SVN (SVN-L) seen with the visible spectrum is lower in the control limbs than in CEAP C_1 limbs ($p < .001$). Although the infrared images allow the visualisation of a greater percentage of SVN-L in both groups of limbs, the differences between groups disappear except in the lateral lower leg ($p = .016$, Mann–Whitney U test). ATh = anterior thigh; MTh = medial thigh; LTh = lateral thigh; PTh = posterior thigh; ML = medial lower leg; LL = lateral lower leg; PL = posterior lower leg.

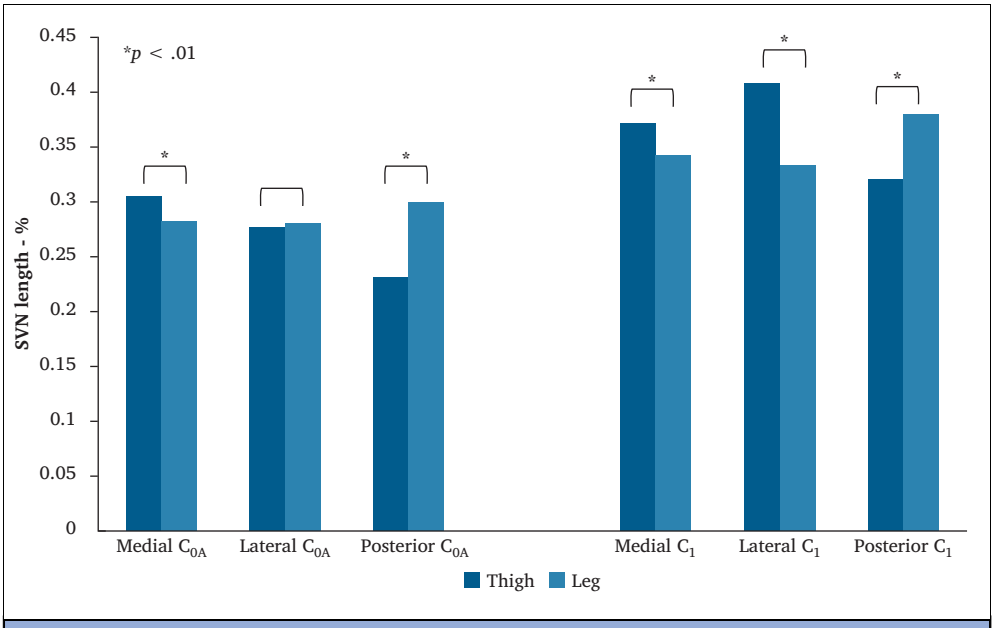

Figure 7. Graphical representation of the percentage of subcutaneous venous network (SVN) extent seen, grouped by adjacent anatomical areas and by group of patients (values expressed as median). The SVN of each of the different sides of the lower extremity (lateral, posterior, and medial) of both the thigh and the lower leg presents many connections (see Supplementary Material). Given that the general conditions of each patient should act in a similar way on all anatomical regions of the lower extremity, one would expect that the proportion of SVN visualised by infrared illumination would be the same in these associated areas. However, this graph shows that the median SVN length is statistically different in each group of subjects grouped by anatomical area. *$p < .01$ (Wilcoxon test).

Table 2. Superficial venous network diameters obtained from both the best contrasted and wider veins from each anatomical area and each group of limbs (infrared images)

Anatomical area	*n*	Superficial venous network diameter − mm		*p* value
		Median (IQR)	Range	
Anterior thigh				
C_{0A}	100	2.7 (2.2–3.8)	1.3–4.7	<.001
C_1	118	6.6 (5.3–9.7)	2.4–12.5	
Medial thigh				
C_{0A}	100	3.3 (2.2–4.2)	1.3–6.3	<.001
C_1	118	6.4 (4.6–6.8)	3.7–11.0	
Lateral thigh				
C_{0A}	100	2.6 (2.2–3.7)	1.2–6.1	<.001
C_1	118	6.1 (4.6–8.2)	2.1–13.0	
Posterior thigh				
C_{0A}	100	2.3 (1.8–3.0)	0.4–5.4	<.001
C_1	118	5.3 (4.2–7.1)	2.3–16.0	
Lateral lower leg				
C_{0A}	100	2.8 (1.8–3.6)	0.6–5.1	<.001
C_1	118	5.6 (4.1–6.7)	2.5–12.2	
Medial lower leg				
C_{0A}	100	2.6 (1.9–3.4)	1.1–5.5	<.001
C_1	118	5.9 (3.9–7.3)	2.6–15.2	
Posterior lower leg				
C_{0A}	100	3.2 (1.8–4.3)	1.2–5.7	<.001
C_1	118	5.3 (3.4–7.6)	1.6–14.0	

IQR = interquartile range.

and the CEAP classification uses those diameters to establish the boundary between C_1 and C_2. As in NIr-I images the boundaries between the SVN and the surrounding tissue are sharper, the measurement of the diameters can be done more accurately than with the naked eye. Table 2 shows that the median SVN diameters of C_{0A} limbs range from 2.3 to 3.3 mm so they are at the upper limit of the visual scale, while the C_1 diameters range from 5.7 to 7.4 mm. As expected, the SVN diameters of C_1 limbs are higher than those of C_{0A} limbs in all anatomical areas. This finding, together with the fact that the *SVN-L* shown by NIr-I does not differ substantially between C_{0A} limbs and C_1 limbs (Fig. 6), suggests that the change in the SVN in C_1 limbs occurs by dilation of pre-existing veins. It is possible that some dilation could be present in C_{0A} limbs, hidden from the naked eye but revealed by the IrS. This requires further research, including C_{0A}, C_{0S}, C_1, and even C_2 — C_4 limbs, with two objectives: to match the limit values used in direct vision scans and those studied by NIr-I, and know the characteristics of the SVN, including its diameter, in the different CEAP clinical classes. These studies will indicate whether it will be necessary to modify the criteria used to differentiate between pathological reticular veins and varicose veins (3 mm in diameter). The use of larger samples will determine whether SVN characteristics are influenced by other factors such as body mass index or age.

From a practical point of view, the NIr-I allows immediate visualisation of the SVN, even in patients with darker skin types, facilitating treatment planning. It may also help to

understand changes over time, either spontaneously or after sclerotherapy. From a research point of view, it will allow the morphological characteristics and diameters of the SVN in all clinical (C) classes of the CEAP classification to be known. Perhaps, along with functional studies, this can contribute to redefinition of its parameters.

Study limitations

The sample contained only women, for two fundamental reasons. Firstly, few men seek advice for tiny visible veins (CVD CEAP C_1 class), making it difficult to include a significant number of male subjects; and, secondly, leg hair, when numerous or very pigmented, reduces the capacity of infrared light to detect the SVN (Fig. S8; Supplementary Material). Unfortunately, in this study, patients in the C_{0A} group were significantly younger and the role of age cannot be excluded. Other limitations, such as the distance between the SVN and the skin, vein diameter, or skin colour, have been analysed previously.[15]

CONCLUSION

This investigation confirms that NIr-I is a useful tool with which to obtain information on the morphological characteristics of the SVN, allowing a field of visualisation greater than that perceivable by the naked eye. This capacity was detected in both the C_1 and C_{0A} groups. Qualitatively, in relation to the C_{0A} limbs, irregular diameters, trajectories, and colourations seem to be the main characteristics of the SVNs of C_1 limbs. Quantitatively, the greater diameter of the SVNs from C_1 CEAP limbs seem to be an important variable to study. Further investigations are needed in order to explore the possibilities.

CONFLICTS OF INTEREST

None.

FUNDING

None.

APPENDIX A. SUPPLEMENTARY DATA

Supplementary data to this article can be found online at https://doi.org/10.1016/j.ejvs.2019.11.034.

REFERENCES

1 Eklof B, Rutherford RB, Bergan JJ, Carpentier PH, Gloviczki P, Kistner RL, et al. Revision of the CEAP classification for chronic venous disorders: consensus statement. *J Vasc Surg* 2004;**40**:1248–52.
2 Wittens C, Davies AH, Baekgaard N, Broholm R, Cavezzi A, Chastanet S, et al. Editor's Choice. Management of chronic venous disease. Clinical practice guidelines of the European Society for Vascular Surgery. *Eur J Vasc Endovasc Surg* 2015;**49**:678–773.
3 Coleridge-Smith P, Labropoulos N, Partsch H, Myers K, Nicolaides A, Cavezzi A. Duplex ultrasound investigation of the veins in chronic venous disease of the lower limbs—UIP consensus document. Part I. Basic principles. *Eur J Vasc Endovasc Surg* 2006;**31**:83–92.
4 Somjen GM, Ziegenbein R, Johnston AH, Royle JP. Anatomical examination of leg telangiectases with duplex scanning. *J Dermatol Surg Oncol* 1993;**19**:940–5.
5 Govind D, Thomas KN, Hill BG, van Rij AM. Microvenous reflux in the skin of limbs with superficial venous incompetence. *Ultrasound Med Biol* 2018;**44**:756–61.
6 Imanishi N, Kishi K, Chang H, Nakajima H, Aiso S. Three-dimensional venous anatomy of the dermis observed using stereography. *J Anat* 2008;**212**:669–73.
7 Vincent JR, Hill GB, van Rij AM. Failure of microvenous valves in small superficial veins is a key to the skin changes of venous insufficiency. *J Vasc Surg* 2011;**54**:62S–9S.
8 Agus GB, Allegra C, Antignani PL, Arpaia G, Bianchini G, Bonadeo P, et al. Guidelines for the diagnosis and therapy of the veins and lymphatic disorders. *Int Angiol* 2005;**24**:107–68.
9 Jawien A, Grzela T, Ochwat A. Prevalence of chronic venous insufficiency in men and women in Poland: multicenter cross-sectional study in 40095 patients. *Phlebology* 2003;**18**:110–22.
10 Chiesa R, Marone EM, Limoni C, Volonte M, Schaefer E, Petrini O, et al. Chronic venous insufficiency in Italy: the 24-cities-cohort study. *Eur J Vasc Endovasc Surg* 2005;**30**:422–9.
11 Rabe E, Guex JJ, Puskas A, Scuderi A, Fernández-Quesada F. The VCP Coordinators. Epidemiology of chronic venous disorders in geographically diverse populations: results from the Vein Consult Program. *Int Angiol* 2012;**31**:105–15.
12 Kern P. Sclerotherapy of telangiectasias: a painless two-step technique. *Dermatol Surg* 2012;**38**:860–4.
13 Kourkoumelis N, Tzaphilidou M. Medical safety issues concerning the use of incoherent infrared light in biometrics. In: Kumar A, Zhang D, editors. *Ethics and Policy of Biometrics*. Berlin: Springer-Verlag; 2010. p. 121–6.
14 Yen K, Gorelick MM. New biomedical devices that use near-infrared technology to assist with phlebotomy and vascular access. *Pediatr Emerg Care* 2013;**29**:383–5.
15 Zharov VP, Ferguson S, Eidt JF, Howard PC, Fink LM, Waner M. Infrared imaging of subcutaneous veins. *Lasers Surg Med* 2004;**34**:56–61.
16 de Zeeuw R, Noordmans HJ, Verdaasdonk RM, Wittens CHA. Objective non-invasive technique for quantification of superficial varicose veins. *Phlebology* 2005;**20**:60–2.
17 Bustos LL, Fronek A, López-Kapke BA, Henríquez JA. Nonvisible insufficient subcutaneous reticular venous plexus can be observed through the skin using a new illumination method. *Dermatol Surg* 2010;**36S**:1046–9.
18 Jefatura del Estado Español. Ley 14/2007 de Investigación Biomédica. BOE 2007;159:28826-28848. (Head of the Spanish State. Law 14/2007 of Biomedical Research. BOE 2007;159:28826-28848).
19 Shahzad A, Saad MN, Walter N, Malik AS, Meriaudeau F. Hyperspectral venous image quality assessment for optimum illumination range selection based on skin tone characteristics. *Biomed Eng Online* 2014;**13**:109.
20 Sinthanyothin C, Boyce JF, Cook HL, Williamson TH. Automated localization of the optic disc, fovea, and retinal blood vessels from digital colour fundus images. *Br J Ophthalmol* 1999;**83**:902–10.
21 Haxthausen H. Infra-red photography of subcutaneous veins. *Br J Dermatol* 1933;**45**:506–11.
22 Scott HJ, Coleridge-Smith PD, McMullin GMM, Scurr JH. Venous disease: investigation and treatment, fact or fiction? *Ann R Coll Surg Engl* 1990;**72**:188–92.
23 Kim M, Park J, Rhee N, Je SM, Hong SH, Lee YM, et al. Efficacy of VeinViewer in pediatric peripheral intravenous access: a randomized controlled trial. *Eur J Pediatr* 2012;**171**:1121–5.
24 Kaddoum R, Anghelescu D, Parish M, Wrigt BB, Trujillo L, Wu J, et al. A randomized controlled trial comparing the AccuVein AV300 device to standard insertion technique for intravenous cannulation of anesthetized children. *Paediatr Anaesth* 2012;**22**:884–9.
25 Taylor GI, Caddy CM, Watterson PA, Crock JG. The venous territories (venosomes) of the human body: experimental study

and clinical implications. *Plast Reconstr Surg* 1990;**86**:185–213.

26 Wilson EE. The changes in Infra-red photographs taken during the treatment of varicose veins. *Am J Surg* 1937;**37**:470–4.

Eur J Vasc Endovasc Surg (2020) 59, 634

COUP D'OEIL

Chronic Limb-Threatening Ischaemia with Aortic Saddle Embolus Treated by Percutaneous Mechanical Thrombectomy

Arindam Chaudhuri *, **Ramita Dey**
Bedfordshire—Milton Keynes Vascular Centre, Bedford Hospital NHS Trust, Bedford, UK

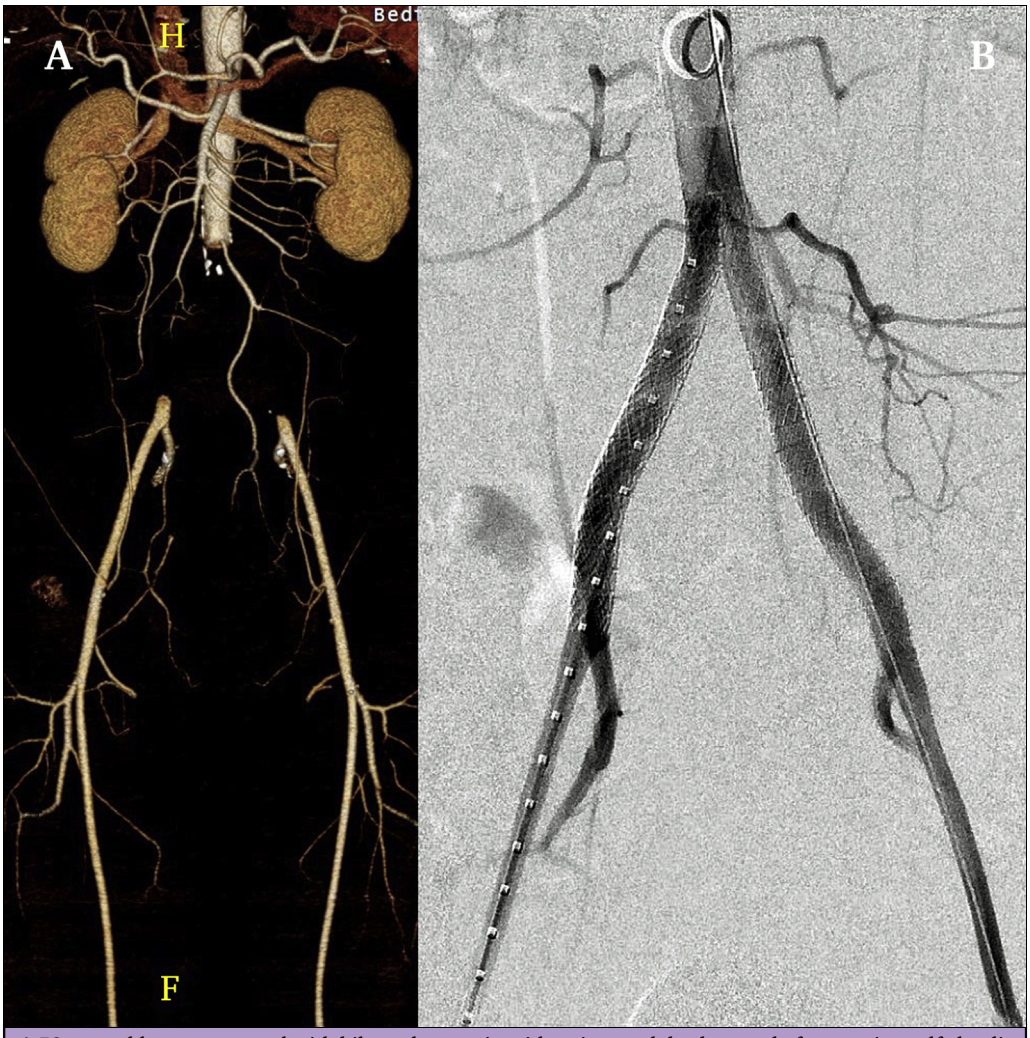

A 58-year-old man presented with bilateral rest pain with a six month background of worsening calf claudication. Computed tomography angiography revealed occlusive saddle embolus at the aortic bifurcation up to the inferior mesenteric artery origin (A), and also left ventricular thrombus. Bilateral percutaneous thrombectomy using an 8 F Rotarex catheter (Straub, Wangs, Switzerland) largely cleared the iliac circuits and distal abdominal aorta. (B) Bilateral kissing stent grafts (VBX 8 mm; W.L Gore & Associates, Flagstaff, AZ, USA) were deployed to cage residual thrombus with symptom resolution. The patient is maintained on clopidogrel and edoxaban (to treat the left ventricular thrombus) and remains asymptomatic at two months.

* Corresponding author. Bedfordshire—Milton Keynes Vascular Centre, Bedford Hospital NHS Trust, Kempston Road, Bedford, MK42 9DJ, UK.
E-mail address: a.chaudhuri@ntlworld.com (Arindam Chaudhuri).
Twitter: @vascularis

https://doi.org/10.1016/j.ejvs.2019.12.021